OPEN ACCESS
Journal of Innovative Optical Health Sciences
Vol. 16, No. 3 (2023) 2330006 (13 pages)

DOI: 10.1142/S1793545823300069

World Scientific
www.worldscientific.com

Three-dimensional structure of liver vessels and spatial distribution of hepatic immune cells

Mengli Xu*, Zheng Liu*, Xinlin Li†, Xinru Wang†, Xuenan Yuan†, Chenlu Han† and Zhihong Zhang*,†,‡

*Key Laboratory of Biomedical Engineering of Hainan Province, School of Biomedical Engineering, Hainan University, Haikou, Hainan 570228, P. R. China

†Britton Chance Center and MoE Key Laboratory for Biomedical Photonics, Wuhan National Laboratory for Optoelectronics-Huazhong University of Science and Technology, Wuhan, Hubei 430074, P. R. China

‡zhzhang@hainanu.edu.cn

Received 15 December 2022
Accepted 1 March 2023
Published 14 April 2023

As the largest internal organ of the human body, the liver has an extremely complex vascular network and multiple types of immune cells. It plays an important role in blood circulation, material metabolism, and immune response. Optical imaging is an effective tool for studying fine vascular structure and immunocyte distribution of the liver. Here, we provide an overview of the structure and composition of liver vessels, the three-dimensional (3D) imaging of the liver, and the spatial distribution and immune function of various cell components of the liver. Especially, we emphasize the 3D imaging methods for visualizing fine structure in the liver. Finally, we summarize and prospect the development of 3D imaging of liver vessels and immune cells.

Keywords: Liver; blood vessel; immune cell; 3D imaging.

1. Introduction

The liver plays an important metabolic and detoxifying function. The liver contains a dense vascular system,[1] and a large number of hepatocytes and immune cells are closely arranged between the liver sinusoids. The study of the three-dimensional (3D) spatial distribution of the liver vascular system and immune cells is necessary for exploring the mechanism of liver disease. This review highlights recent advances in 3D imaging of the structure and composition of the liver vascular system and immune cells. The main contents cover advances in imaging of the liver vascular circulatory system, the 3D anatomical structure of the liver

‡Corresponding author.

circulatory system at different scales, the distribution and function of immune cells in the liver, and the 3D imaging methods for liver immune cells.

2. Structure of the Liver Vascular System and its Imaging Methods

The liver is located below the diaphragm in the abdominal cavity of the human body,[2] and it is divided into the left lobe and right lobe according to the distribution of the vascular. Moreover, the liver is further divided into eight segments according to Couinaud's liver segments method, with segments 1–4 being located in the left lobe, and segments 5–8 being located in the right lobe (Fig. 1).[3] The mouse liver is segmented into five lobes according to morphology and distribution, including left lateral lobe, median lobe, right anterior lobe, right posterior lobe, and caudate lobe. The liver has a complex vascular network, including bile ducts, and blood and lymphatic vascular networks. Although the macrovascular structure of the liver is well understood, the features of the microcirculation (hepatic sinusoids) remain unclear.

2.1. *The vascular network of the liver*

The liver is a highly vascularized organ with blood circulating 12 times per hour.[2,4] The vascular network is composed of hepatic veins (HV), portal veins (PV), and hepatic arteries (HA), which are connected by hepatic sinusoids with an average diameter of 5–14 μm (Fig. 2).[5] Liver cells are essential for blood detoxification, and the liver receives 75% of the blood from the PV, which delivers nutrients and toxins from peripheral organs, including the intestine, spleen, pancreas, etc. The remaining 25% of the blood comes from the HA, which originates from the celiac artery and supplies oxygen to the liver. The peripheral blood flows from the PV and HA, and enters into the central vein (CV) *via* the hepatic sinusoids, and then forms HV that will drain into the inferior vena cava.

In the vascular network of the liver, the hepatic sinusoids serve as the capillaries of the liver. The hepatic lobule is the basic structural unit of the liver, and hepatic sinusoids constitute a honeycomb network in the hepatic lobule. Besides hepatic parenchymal cells and liver sinusoid endothelial cells (LSECs), the liver has a variety of immune cell components. The cross-section of the human hepatic lobule is hexagonal,[6] and the border areas are distributed with portal triads formed by interlobular veins, interlobular arteries, and interlobular bile ducts.[7,8] The center of the hepatic lobule is the CV formed by the branches of the HV. The radiating hepatic sinusoid in the hepatic lobule connects the hepatic PV and HA through the interlobular vein and interlobular artery.[8] Interestingly, latest research showed that the hepatic lymphatic vessels are also distributed at the portal area and closely entangled with the PV (Fig. 2(a)).[9]

2.2. *The basic structural units of the liver*

The theory of hexagonal hepatic lobule was first proposed by Kiernan in 1833. It describes the widely accepted microstructure of the liver microanatomical.[10] This model features the CV in the middle of the classical hepatic lobule, which is the terminal branch of the HV. The portal triads are composed of

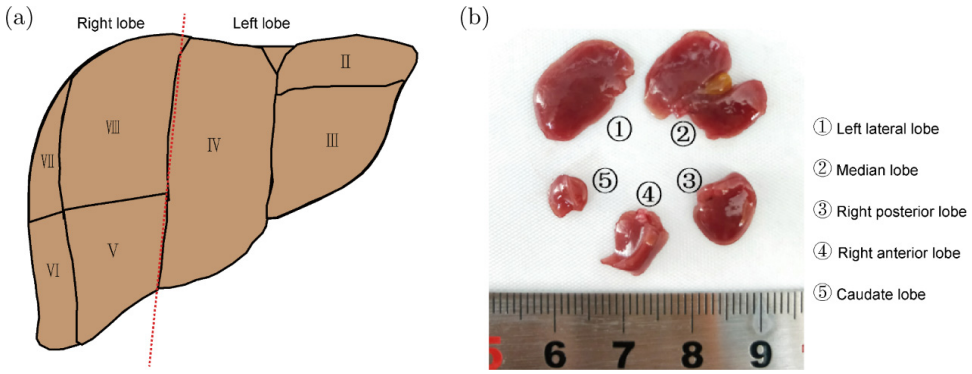

Fig. 1. Segments and lobulation of the liver. (a) Schematic diagram of the human liver. The liver is divided into two lobes, left and right, with eight segments, of which the back of segment IV is segment I. (b) Picture of mouse liver, divided into five liver lobes.

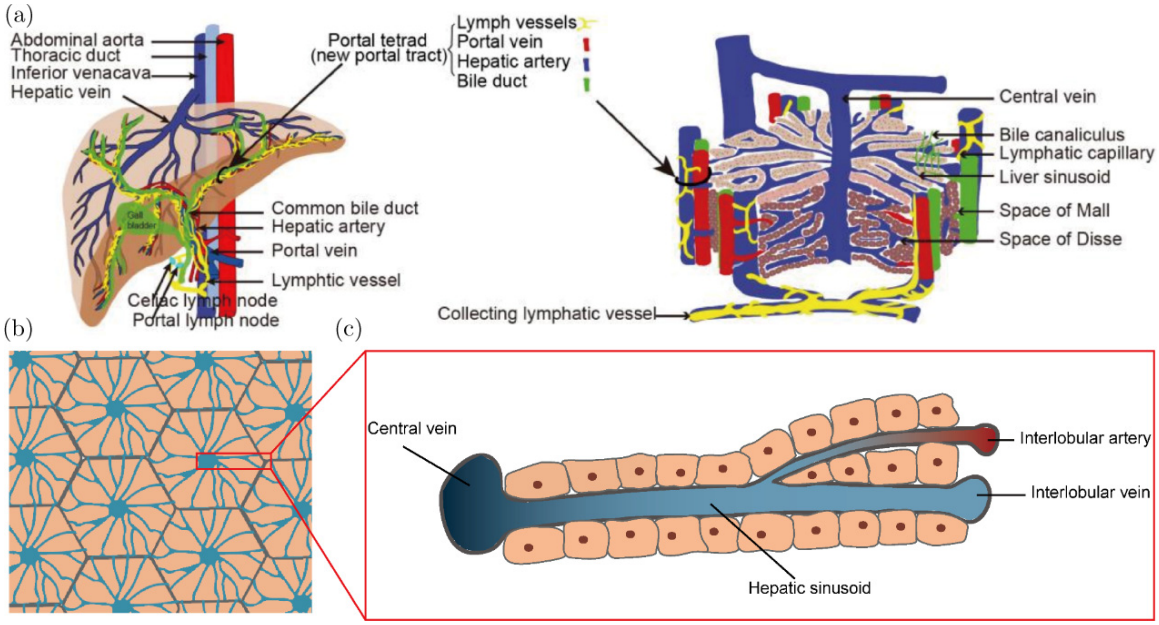

Fig. 2. Schematic diagram of the composition of the liver vasculature. (a) Schematic diagram of the liver.[9] (b) Schematic diagram of the hexagonal hepatic lobule. Blue: CVs and liver sinusoids. (c) Schematic of the intersection of the interlobular veins and the interlobular arteries at the hepatic sinusoids. Red: interlobular arteries. Blue: interlobular veins, hepatic sinusoids, CVs.

the PV, HA, and bile duct, and the portal triads are distributed at the junction of two classical hepatic lobules. However, the hexagonal hepatic lobule oversimplifies the complex lobular structure of the liver. The shape of the hepatic lobules of mice is not hexagonal columns as is generally considered. *In vivo* photoacoustic imaging clearly revealed that the criss-crossing arrayed hepatic lobules were not in regular shape. The structure of hepatic sinusoids in the hepatic lobule presented complex labyrinthine networks, rather than regular radial distribution.[11] The latest research showed that the mouse hepatic lobules tended to be oblate ellipsoids, as revealed by liver-CUBIC optical clearing approach.[5] In addition, as shown in Fig. 3, according to the distribution of hepatic vascular branches, the structural units of the liver can also be defined as the portal lobule (where the PV and bile duct are located at the center, CV at the boundary)[12] and the hepatic acinar structure (where the PV as the central axis and CV at both ends).[13]

2.3. *Anatomical 3D imaging of hepatic vessels*

Fueled by the development of imaging technology, the method for liver vessel imaging has significantly improved. In addition to conventional 2D imaging, the 3D imaging of the hepatic vascular network offers more informative and complete pathological data. As early as the 1950s, German doctor Claude Couinaud divided the complete human liver into eight segments according to the branching direction of the hepatic vessels.[14,15] Couinaud's liver segment theory is regarded as the beginning of the era in liver surgery, and it's an important milestone in the anatomy of the intact hepatic vascular system. This segment theory has become a common clinical practice for doctors.[3]

Digital human database

For achieving a comprehensive view of the 3D anatomical structure in humans, the American Visual Human Project (VHP) obtained a complete digital human database (2048 × 1216 pixels) set by sequential cutting at intervals of 1 mm and 0.33 mm in the 1990s. The VHP presented the 3D anatomical atlas of individual organs to human beings. In 2002, the first Chinese Visible Human (CVH) database in China was obtained through an improved scheme, and the human body data was collected with a more advanced Computer Numerical Control (CNC) milling machine at intervals of 0.1–1 mm. The digital photography resolution of its cross-section was 3072 × 2048 pixels.[16] In comparison with the previous VHP database, CVH database offered higher resolution and better integrity enabling it to

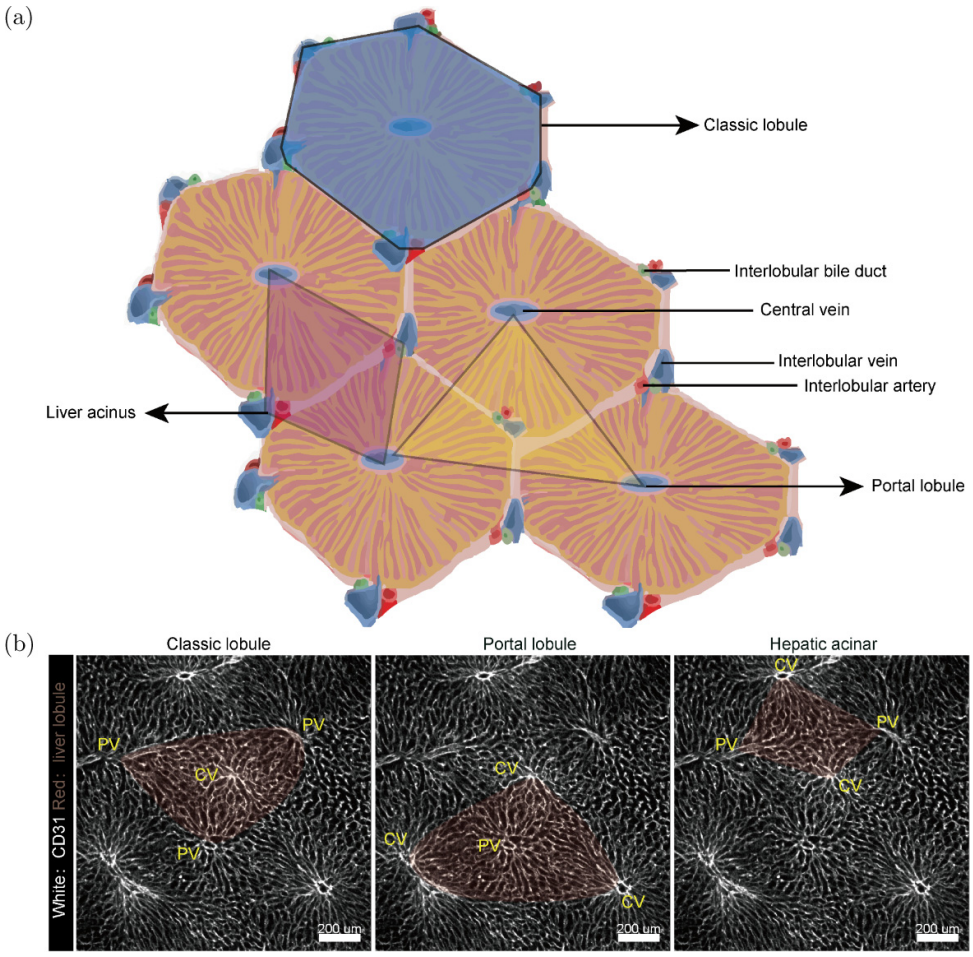

Fig. 3. The structure of hepatic lobules. (a) Schematic diagram of the classical hepatic lobule, portal lobule, and hepatic acinus. The light blue pseudo-color area circled the classical hepatic lobule, the light yellow pseudo-color area circled the portal lobule, and the magenta pseudo-color area circled the hepatic acinar. (b) The sinusoidal structure in the classical lobule, normal portal lobule, and the hepatic acinar.[5]

provide more precise information on the 3D anatomical structure of liver vessels. For example, Chen *et al.* reconstructed the HV, PV, HA, and bile duct of the human liver based on the CVH database, which provided a complete digital model of liver vascular anatomy.[17] CVH database is an invaluable resource for the study of human liver anatomy and clinical practice. In 2017, the published Human Digital Liver Databank displayed the 3D models of healthy or diseased livers that provided a valuable platform for the study of liver structure.[18]

Liver anatomy imaging by CT and MRI

Computed tomography (CT) and magnetic resonance imaging (MRI), which developed in the 1970s and 1980s, have become widely used in clinical practice due to their ability to achieve liver vascular structure at 0.5–2 mm resolution. These techniques have greatly contributed to uncovering the 3D structure of large liver vascular and bile duct, advancing the diagnosis of liver diseases and aiding in preoperative assessment of patients.[19] However, limited by the background noise interference in CT and MRI imaging of the liver, the accurate reconstruction of liver vessels from 3D imaging data remains full of challenges. Recently, Zeng *et al.* achieved an effective identification and segmentation of HV and PV with a specificity, average accuracy, and sensitivity of 98.6%, 97.7%, and 79.8% through the combination of oriented flux symmetry and graph cuts.[20] Goceri *et al.* proposed a fully automated and adaptive method to segment hepatic PV and HV in MRI imaging data.[21] Deep learning networks also play an important role in the segmentation of hepatic vessels.[22–24] Moreover, some software for hepatic vascular segmentation and 3D printing techniques have also been

developed for the 3D reconstruction of the liver blood vessels and lesion structure based on the CT and MRI data of patients.[25,26]

Liver high-resolution anatomy imaging by micro-CT and photoacoustic imaging

Furthermore, limited by the resolution of CT and MRI techniques, most vascular segmentation methods only provided macroscopic anatomical information for the 3D imaging of liver vessels. The emergence of micro-computer tomography (micro-CT) in scientific research has enhanced the imaging resolution of liver vessels. For example, Debbaut *et al.* performed vascular imaging and reconstruction of macrovascular to microcirculation in the human liver by a combination of vascular corrosion casting and micro-CT imaging.[27] They analyzed the radius, length, and number of vessel branches for the HV, PV, and HA. Although the micro-CT is ideal in the imaging of the macro- and mesoscale vascular system of the human liver, the characterization of sinusoidal connectivity is unsatisfying during microcirculation imaging. Peeters *et al.* combined vascular corrosion casting and micro-CT imaging to reconstruct 3D blood vessels in rat liver, with an imaging resolution of 40 μm. This approach enabled the realization of 3D imaging of the PV, HV, and HA in intact rat liver.[28] These studies showed that the average diameter of the HA was thinner than the PV, and the PV was thinner than the HV. The HA and PV were found to lay parallel to each other. In 2018, Peeters *et al.* conducted a thioacetamide (TAA)-induced liver cirrhosis rat model to quantitatively analyzed the 3D distribution of blood vessels in the liver.[29] This study found that liver cirrhosis induced an irreversible effect on the liver vascular morphology, resulting in vessels appearing to collapse or sudden sharp bends. Hankeova *et al.* developed a double resin casting micro-computed tomography (DUCT) method, which achieved imaging of hepatic bile ducts and vessels in an intact liver lobe (Fig. 4(a)).[30] However, due to the viscosity of the resin, the DUCT did not recognize vessels smaller than 5 μm, which was

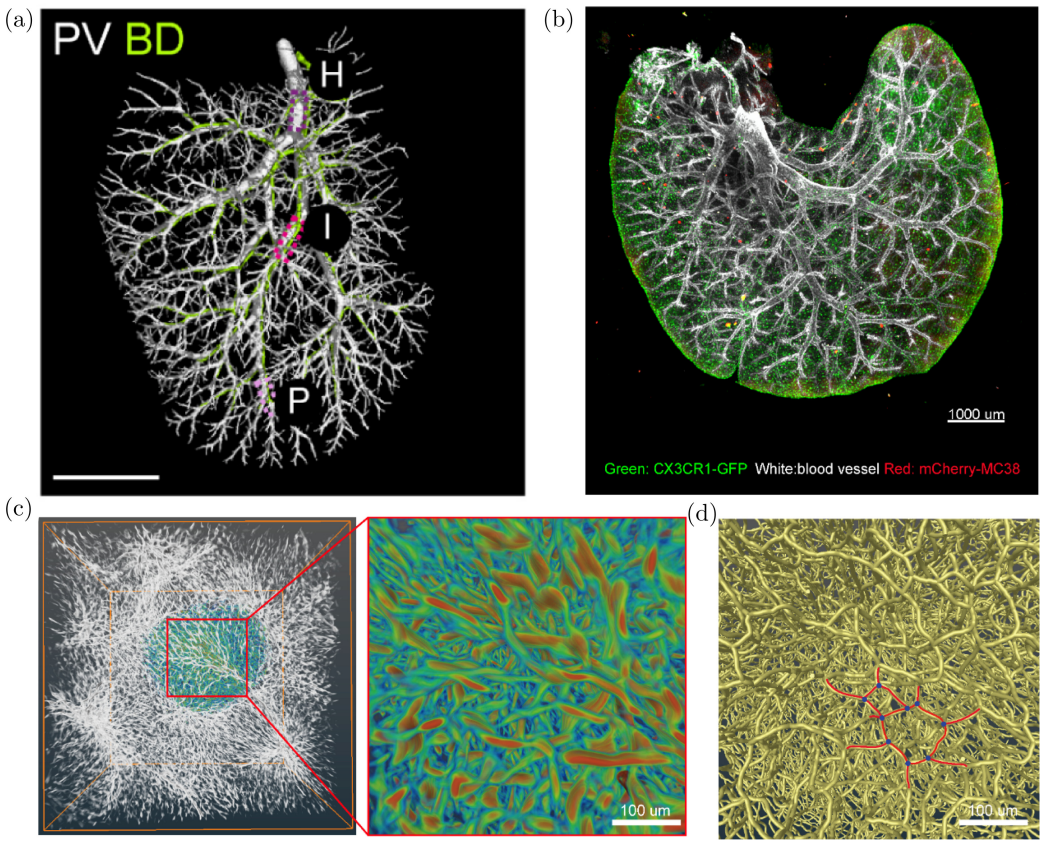

Fig. 4. Optical clearing and imaging of the liver.[5,42] (a) 3D reconstruction of the PV and bile duct (BD) of a mouse liver by micro-CT. White: PV, green: BD. Scale bar: 4 mm. (b) The intact liver lobe imaging for TH immunolabeling by light-sheet imaging. (B) The confocal imaging of the liver lobe with colorectal micrometastases. (c and d) The 3D imaging and skeleton of hepatic sinusoids.

insufficient for large-volume imaging of hepatic sinusoids. Lin *et al.* acquired the fine spatial distribution of hepatic sinusoids in the mouse liver by *in vivo* photoacoustic imaging, and the liver lobule was clearly visible from the liver capsule.[11] However, the image depth of photoacoustic imaging was affected by resolution. The cross-sectional image data indicated that the image depth of photoacoustic imaging for the hepatic sinusoids was limited to 300 μm.

2.4. *Optical microscope imaging of liver structure at single-cell resolution*

Although the above-mentioned 3D imaging methods of liver vessels achieved fast speed and large-volume imaging of liver structure, their resolution limited the obtaining of intact liver structure information at single-cell resolution with high accuracy. Confocal, multiphoton, and photoacoustic imaging techniques have realized single-cell resolution imaging of the liver tissue.[31–33] These techniques can acquire dynamic information from *in vivo* imaging data with significant implications for understanding the motor behavior and function of the immunocytes. Yu *et al.* demonstrated that α-melittin-NPs targeted the LSECs *in vivo via* confocal imaging.[34] Lin *et al.* visualized the 3D distribution of KC and hepatic sinusoids *viain vivo* photoacoustic and fluorescence imaging.[11] Liu *et al.* investigated the dynamic molecular events in CTLs killing metastatic tumor cells in the liver *via* real-time confocal imaging.[35] However, the liver is dense with a high level of lipid and pigment contents, making it difficult for light to penetrate liver tissue, and the confocal imaging depth is less than 100 μm. Therefore, confocal or multiphoton can only be used for small volume imaging of the liver. For example, Hammad *et al.* performed a small volume 3D imaging of hepatic sinusoids, bile canalicular, and hepatocytes under 100 μm thick liver tissue by confocal 3D scanning.[36] Although photoacoustic imaging technology has improved the imaging depth of liver tissue by optical microscopy,[37] its development is limited by the development of photoacoustic probes and the dense vascular structure of the liver, and it has yet to achieve intact liver structure at single-cell resolution. Recently, the development of microscopic optical tomography and tissue transparency enabled researchers to obtain the 3D structure of hepatic vascular, duct, immunocytes, and neurons in intact livers.

Optical clearing of liver

To address the limitations of confocal microscopic imaging in achieving deeper liver imaging, recent advancements in optical clearing methods reduce tissue absorptivity and scattering, enabling increased light penetration depth.[38,39] This makes it possible for noninvasively image large or even intact liver vasculature networks. For example, Oren *et al.* performed confocal imaging of the liver of $\mathrm{Vecad}^{\mathrm{cre}}$/$\mathrm{tdTomato}^{\mathrm{fox/stop/fox}}$ transgenic mice, which specifically labeled the blood vessels. By combining the optical clearing methods of Clarity and ScaleA2, they obtained a single cell resolution vascular image of 1200 μm × 600 μm × 600 μm that clearly distinguished the spatial distribution information of hepatic sinusoids in hepatic lobules.[40] Jing *et al.* used the PEGASOS optical clearing method in combination with confocal microscopic imaging technology to achieve 3D imaging of complete hepatic lobe vessels in Tie2-Cre; Ai14 mice that specifically label hepatic blood vessels.[41] However, due to the influence of transparency or background fluorescence, the overall resolution of hepatic sinusoids is poor,

Table 1. Summary table of liver anatomy 3D imaging.

Imaging method	Resolution	Imaging characteristic
CNC cutting and digital photography	0.1–1 mm	Realize the acquisition of complete human anatomy data. The data collection is relatively comprehensive and the resolution is not high. Imaging for fixed samples, not live samples.
CT	0.5–1.5 mm	Widely used in clinical diagnosis. Realize rapid scanning and imaging of all organs of the body, and the resolution is not high.
MRI	0.5–2 mm	Widely used in clinical diagnosis. Realize rapid scanning and imaging of all organs of the body, and the resolution is not high.
micro-CT	1–100 μm	Mostly used in scientific research with high resolution and a relatively limited imaging range.
Photoacoustic imaging	3–100 μm	Realize intravital imaging, and the image depth was affected by resolution.

and it is difficult to analyze the network topology of hepatic sinusoids. Adori *et al.* and Liu *et al.* used the iDISCO 3D immunoimaging to obtain 3D neural distribution in the liver, and explore the distribution change of the liver nervous system in disease.[42,43] To overcome the problem of liver transparency and fluorescence retention, Liu *et al.* developed a fast and fluorescence-preserving transparency method, liver-CUBIC, to achieve single-cell resolution imaging of the vascular structure in intact liver lobes (Fig. 4(b)).[5] The liver-CUBIC method analyzed the topological change of hepatic sinusoids in normal and diseased conditions, providing an important scheme to study the 3D fine vascular structure of the liver (Fig. 4(c)).

Thus, the combination of optical clearing methods with optical microscope imaging provides high-resolution imaging, which can obtain not only the main vascular branches of the liver but is also suitable for the large-volume imaging of hepatic sinusoids. This approach is an effective method for realizing the 3D imaging of the hepatic vascular network. However, it requires long imaging time, high imaging equipment, and fine transparency of the liver tissue. For larger liver samples, such as the liver in primates, optical clearing technology is required to be more effective and the imaging equipment should have a long working distance.

Micro-optical sectioning tomography imaging

To overcome the limited depth of confocal imaging in liver tissue, researchers have developed a method of cutting the liver into thin slices, followed by sequential imaging and reconstruction. For example, Takashima *et al.* achieved 3D reconstruction of $800\,\mu\text{m} \times 800\,\mu\text{m} \times 500\,\mu\text{m}$ hepatic portal vein and hepatic bile duct by layer-by-layer cutting and confocal imaging (resolution: $0.62\,\mu\text{m} \times 0.62\,\mu\text{m} \times 10\,\mu\text{m}$), enabling the study the periportal bile duct development.[44] In addition, the fluorescence micro-optical sectioning tomography (fMOST) system that based on continuous cutting imaging and data reconstruction, has been reported as an effective method for large-volume imaging of the intact murine liver lobe ($9786\,\mu\text{m} \times 8640\,\mu\text{m} \times 10,312\,\mu\text{m}$). This system achieved subcellular resolution ($0.32\,\mu\text{m} \times 0.32\,\mu\text{m} \times 1\,\mu\text{m}$) imaging of embedded biological samples for 3D data reconstruction (Fig. 5).[45]

It should be noted that two-photon or confocal imaging of liver microcirculation dynamics is mainly used in anesthetized animals or in explanted, non-perfused livers. These data provide limited information about hemodynamics or immunocyte behavior in a living individual, especially in the human liver. Therefore, it remains a significant challenge to monitor liver microcirculation dynamics and/or immune cell migration in humans *via* noninvasive imaging approaches. Recently, side-stream dark field (SDF) has been used to measure post-reperfusion hepatic microcirculation and sinusoid density in clinical liver transplantation. This imaging method provides real-time information on microcirculatory dysfunction during early allograft dysfunction.[46] One disadvantage is that the SDF approach necessarily requires invasiveness at this stage, but it has utility intra-operatively for selecting donor's liver.

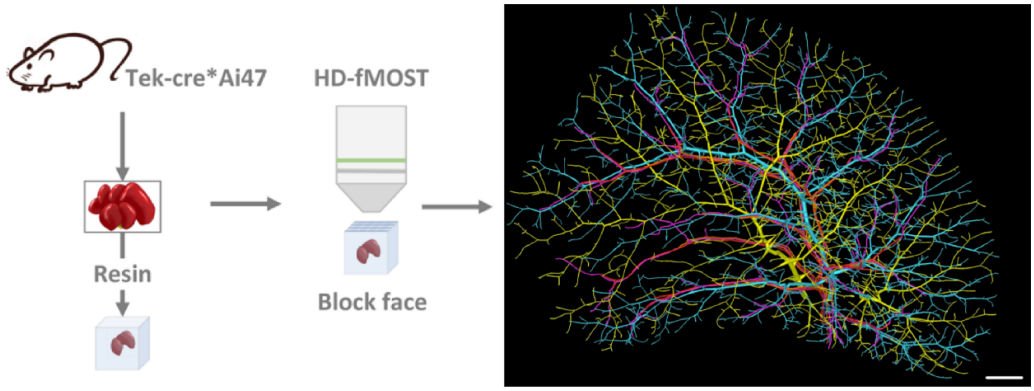

Fig. 5. The intact liver lobe imaging by high-definition fluorescent micro-optical sectioning tomography (HD-fMOST).[45] Cyan: PV, yellow: HV, purple: BD, red: hepatic artery (HA). Scale bar: 1 mm.

Table 2. Summary table of 3D optical microscope imaging of liver at single-cell resolution.

Imaging method	Imaging characteristic
Confocal microscopic imaging	The tissue imaging depth is less than 100 μm, which is more suitable for the acquisition of 2D data.
Frozen section combined with confocal microscopic imaging	The imaging depth can exceed 100 μm, which requires continuous accurate cutting to ensure the integrity of imaging data, and requires high-quality of sample cutting and data reconstruction level.
Optical clearing technology combined with confocal/light-sheet imaging	The imaging depth is generally above 1 mm, and the specific imaging depth is affected by the effect of tissue transparency and the imaging range of imaging equipment.

3. Distribution and Function of Immune Cells in the Liver

The liver comprises various cell types, including hepatic stellate cells (HSCs), Kupffer cells (KCs), lymphocytes, and dendritic cells (DCs), which play an important role in the maintenance of liver homeostasis.[47–49] The tissular location of these hepatic immune cells is related to their function during homeostasis or disease.[50] Extracting the fine structure of the liver is critical for mapping the spatial arrangement of immune cells in the liver, and the analysis of the distribution of the hepatic immune cells is meaningful for understanding their function.

3.1. *Spatial distribution of liver cells*

Taking the blood vessels of the liver as the coordinates, various types of hepatic cells are arranged inside and outside of the liver vascular network.[2,51–53] Among these cells, hepatocytes are the main component of the liver, accounting for $\sim 80\%$ of total liver cells. Hepatocytes are widely distributed outside of hepatic vessels and are critical for liver regeneration, detoxification, and metabolic homeostasis.[51,54,55] The Disse space of the liver lies between the hepatocytes and the hepatic sinusoids. HSCs are located in the perisinusoidal space of Disse with long protuberances and contact with surrounding hepatocytes and hepatic sinusoids.[47] HSCs are involved in the repair response of liver injury and are the main cell types leading to liver fibrosis.[56,57] Additionally, DC cells are distributed in the liver capsular or around large vessels, which plays a role in capturing and processing antigens.[58]

LSECs are the largest population of non-parenchymal cells in the liver, which arranged as monolayer cells in the liver with a sieve-like structure.[2,4,51] They act as a barrier between the liver and blood, continuously sensing and capturing circulating antigens. Recent studies have also found that LSECs play a role in liver regeneration and fibrosis.[59,60] KCs, the largest subsets of resident macrophages in the liver, are distributed in the sinusoidal vascular space and play a vital role in phagocytosis and immune surveillance in the liver.[2,51] They slowly migrate along the hepatic sinusoid, phagocytizing hepatocyte fragments through the fenestrae of the hepatic sinusoid and the space of Disse in a steady-state environment. The latest research results show that KCs are primarily located near the periportal regions of the liver, preventing pathogen transmission in the liver.[61]

Additionally, hepatic lymphocytes have been reported to patrol the hepatic sinusoid[52,62] and maintain the balance of the immune response in the liver.[54] Different subsets of $CD4^+$ T cells exhibit distinct functions in different regions of the liver.[63] For example, Th1 cells accumulate in the portal tracts of biliary atresia or other liver diseases and produce pro-inflammatory cytokines,[64] while Tregs are mainly located in the liver sinusoids and suppress immune responses. Similarity studies have shown that effector $CD8^+$ T cells predominantly distribute in the liver sinusoids and eliminate virus-infected cells,[65] while memory $CD8^+$ T cells patrol the vasculature and rapidly respond to secondary infections.[66,67] Liver-resident $\gamma\delta$T cells, NK cells, and NKT cells are primarily distributed in the hepatic sinusoid, where they contact antigens in the liver stroma through endothelial fenestrae, search for dangerous signals, and secrete cytokines to deal with liver infection and injury.[68–72]

The function and distribution of immune cells in the liver are closely related. For example, DCs and macrophages are strategically located in the liver and constitute a cohesive defense network against

pathogen invasion or clearance of apoptotic hepatocytes. Thus, the physical location of DCs and macrophages as well as their surrounding environment significantly affect their function. Recent studies have highlighted the importance of $CX3CR1^+$ DC subsets that are distributed in the interstitial region for antigen processing and delivery in the liver.[73] $CX3CR1^+CD207^+$ macrophages, located in the hepatic capsule region, can prevent the hepatic dissemination of peritoneal pathogens.[74] $Gpnmb^+Spp1^+$ macrophages are found distributed around the bile duct, but their function in liver disease remains further exploration.[75] KCs distributed inside hepatic sinusoids were able to eliminate circulating pathogens.[76] Therefore, revealing the arrangement of immune cells in the intact hepatic lobe at single-cell resolution will contribute to understanding the function and heterogeneity of immune cells in the liver in the physiological and pathophysiological condition.

3.2. *Imaging of liver cells*

Large-volume imaging of the liver by CT or MRI is hard to achieve the hepatic immune cells at single-cell resolution. The current findings about the distribution of immune cells in the liver are mainly obtained through electron microscope imaging and optical microscopic imaging.[47] Especially, the optical clearing, combined with optical microscopic imaging, not only offers an effective solution for achieving single-cell resolution imaging of hepatic vasculature but also provides an optional way of obtaining 3D spatial distribution data of liver immune cells. For example, uDISCO transparency technology achieves the distribution of transplanted bone marrow stem cells throughout the entire liver lobe at single-cell resolution by light-sheet microscopy,[77] and CUBIC transparency technology achieves the whole-liver imaging of the SUIT-2 cells metastasis model in BALB/c-nu/nu mice utilizing light-sheet microscopy imaging.[78] Apart from that, the liver-CUBIC transparency method enables the simultaneous visualization of immune cells, fine vasculature, and tumor micrometastases in the intact liver lobe by confocal imaging. This approach has facilitated quantitative analyses of the distribution of DC/macrophages in normal, liver fibrosis, nonalcoholic steatohepatitis, and liver metastases models in mice, utilizing liver vessels as coordinates.[5]

4. Summary and Prospect

The noninvasive imaging of intact hepatic vessels *via* CT and MRI has extremely promoted the clinical diagnosis of human liver disease. The imaging of the liver vasculature and immune cells in intact liver at single-cell resolution has improved our understanding of metabolic homeostasis, immunosurveillance, and the hemodynamics of the liver. It should be noted that the optical clear imaging

Table 3. Summary table of spatial distribution and immune function of cells in the liver.

Cell type	Distribution	Main function
Hepatocyte	Widely distributed in the liver, arranged in plates that are distributed among hepatic sinusoids.	Metabolism, protein production, liver toxin neutralization, bile secretion, and liver regeneration.
HSC	Distributed in the space of Disse between hepatocytes and hepatic sinusoids.	Store fat and vitamin A, and participate in liver damage repair and liver fibrosis.
DC	Mainly distributed in the liver capsular or around large vessels. A small amount is distributed in the hepatic lobule.	Capturing and processing of liver antigens
Hepatic endothelial cell	Arranged into monolayer cells and formed a sieve-like hepatic sinusoid structure.	Phagocytosis of antigens in the blood, associated with tumor metastasis, is a prerequisite for liver fibrosis and promotes liver regeneration.
KC	Located inside the sinusoidal vascular space.	The main macrophage population of the liver plays the functions of phagocytosis, immune surveillance, and immune regulation in the liver.
Lymphocyte	A large number of liver lymphocytes are distributed in the hepatic sinusoid.	Plays an immunomodulatory role in liver inflammation, antivirus, tumor immunity, and so on.

approach is an invasive imaging technology that has not been applied to clinical diagnosis without surgery. At present, this approach is mainly used for basic science research in animals and we believed that constantly improved imaging techniques and transparency methods will eventually be used in clinical for assisting pathological diagnostic applications. Meanwhile, obtaining higher-resolution information of vascular and immunocytes in the intact liver through advanced MOST technology will further contribute to the analysis of the hepatic anatomical structure and the uncovering of immune-pathogen crosstalk in the liver.

In the future, continuous exploration of the spatial distribution of hepatic immune cells and the hepatic neuron network in intact liver lobe under physiological and pathophysiological conditions, developing more efficient data processing schemes, and creating more fast and more high-resolution imaging platform will profoundly advance the study of the intrinsic biological mechanism behind liver disease and broaden the avenues for studying the liver anatomy. Moreover, the 3D imaging of the liver combined with the measurement of multi-omics will enable spatial multi-omics with high accuracy and high spatial resolution, which will advance the understanding of the immunocytes' function *in situ*.

Acknowledgments

This work was supported by the National Key Research and Development Program of China (2017YFA0700403), the Hainan University Scientific Research Foundation (KYQD(ZR)20078) and the National Natural Science Foundation of China (81901691). Mengli Xu and Zheng Liu contributed equally to this paper.

Conflict of Interest

The authors declare that there are no conflicts of interest relevant to this paper.

References

1. A. Gibert-Ramos, D. Sanfeliu-Redondo, P. Aristu-Zabalza, A. Martínez-Alcocer, J. Gracia-Sancho, S. Guixé-Muntet, A. Fernández-Iglesias, "The hepatic sinusoid in chronic liver disease: The optimal milieu for cancer," *Cancers* **13**, 5719 (2021).
2. P. Brodt, *Liver Metastasis: Biology And Clinical Management*, Springer, Netherlands (2011).
3. P. Majno, G. Mentha, C. Toso, P. Morel, H. O. Peitgen, J. H. Fasel, "Anatomy of the liver: An outline with three levels of complexity – A further step towards tailored territorial liver resections," *J. Hepatol.* **60**, 654–662 (2014).
4. S. P. S. Monga, *Molecular Pathology of Liver Diseases*, Springer, New York (2011).
5. Z. Liu, M. Xu, S. Huang, Q. Pan, C. Liu, F. Zeng, Z. Fan, Y. Lu, J. Wang, J. Liu, X. Li, Q. Luo, Z. Zhang, "Mesoscale visualization of three-dimensional microvascular architecture and immunocyte distribution in intact mouse liver lobes," *Theranostics* **12**, 5418–5433 (2022).
6. T. Yamaguchi, H. Hachiya, "Modeling of the cirrhotic liver considering the liver lobule structure," *Jpn. J. Appl. Phys.* **38**, 3388–3392 (1999).
7. O. Ohtani, Y. Ohtani, "Lymph circulation in the liver," *Anat. Rec.* **291**, 643–652 (2008).
8. K. B. Halpern, R. Shenhav, H. Massalha, B. Toth, A. Egozi, E. E. Massasa, C. Medgalia, E. David, A. Giladi, A. E. Moor, Z. Porat, I. Amit, S. Itzkovitz, "Paired-cell sequencing enables spatial gene expression mapping of liver endothelial cells," *Nat. Biotechnol.* **36**, 962–970 (2018).
9. S. Huang, B. Li, Z. Liu, M. Xu, D. Lin, J. Hu, D. Cao, Q. Pan, J. Zhang, J. Yuan, Q. Luo, Z. Zhang, "Three-dimensional mapping of hepatic lymphatic vessels and transcriptome profiling of lymphatic endothelial cells in healthy and diseased livers," *Theranostics* **13**, 639–658 (2023).
10. F. Kiernan, "The anatomy and physiology of the liver," *Philos. Trans. R. Soc. Lond. B Biol. Sci.* **123**, 711–770 (1833).
11. Q. Lin, D. Deng, X. Song, B. Dai, X. Yang, Q. Luo, Z. Zhang, "Self-assembled "off/on" nanopomegranate for *in vivo* photoacoustic and fluorescence imaging: Strategic arrangement of kupffer cells in mouse hepatic lobules," *ACS Nano* **13**, 1526–1537 (2019).
12. E. Bhunchet, K. Wake, "The portal lobule in rat liver fibrosis: A re-evaluation of the liver unit," *Hepatology* **27**, 481–487 (1998).
13. A. Rappaport, Z. Borowy, W. Lougheed, "Subdivision of hexagonal liver lobules into a structural and functional unit. Role in hepatic physiology and pathology," *Anat. Rec.* **119**, 11–33 (2010).
14. H. Bismuth, "Surgical anatomy and anatomical surgery of the liver," *World J. Surg.* **6**, 3–9 (1982).
15. H. Bismuth, D. Houssin, D. Castaing, "Major and minor segmentectomies réglées in liver surgery," *World J. Surg.* **6**, 10–24 (1982).

16. S. X. Zhang, P. A. Heng, Z. J. Liu, L. W. Tan, M. G. Qiu, Q. Y. Li, R. X. Liao, K. Li, G. Y. Cui, Y. L. Guo, X. P. Yang, G. J. Liu, J. L. Shan, J. J. Liu, W. G. Zhang, X. H. Chen, J. H. Chen, J. Wang, W. Chen, M. Lu, J. You, X. L. Pang, H. Xiao, Y. M. Xie, "Creation of the Chinese visible human data set," *Anat. Rec. B New Anat.* **275**, 190–195 (2003).
17. G. Chen, S. X. Zhang, L. W. Tan, G. J. Liu, K. Li, J. H. Dong, "The study of three-dimensional reconstruction of Chinese adult liver," *Surg. Radiol. Anat.* **31**, 453–460 (2009).
18. Digital human liver database open platform, http://hdldb.net/en/leader-profile.php.
19. D. Sahani, A. Mehta, M. Blake, S. Prasad, G. Harris, S. Saini, "Preoperative hepatic vascular evaluation with CT and MR angiography: Implications for surgery," *Radiographics* **24**, 1367–1380 (2004).
20. Y. Z. Zeng, Y. Q. Zhao, P. Tang, M. Liao, Y. X. Liang, S. H. Liao, B. J. Zou, "Liver vessel segmentation and identification based on oriented flux symmetry and graph cuts," *Comput. Methods Programs Biomed.* **150**, 31–39 (2017).
21. E. Goceri, Z. K. Shah, M. N. Gurcan, "Vessel segmentation from abdominal magnetic resonance images: Adaptive and reconstructive approach," *Int. J. Numer. Method. Biomed. Eng.* **33**, e2811 (2017).
22. Q. Huang, J. Sun, H. Ding, X. Wang, G. Wang, "Robust liver vessel extraction using 3D U-Net with variant dice loss function," *Comput. Biol. Med.* **101**, 153–162 (2018).
23. T. Kitrungrotsakul, X. H. Han, Y. Iwamoto, L. Lin, A. H. Foruzan, W. Xiong, Y. W. Chen, "VesselNet: A deep convolutional neural network with multi pathways for robust hepatic vessel segmentation," *Comput. Med. Imaging Graph.* **75**, 74–83 (2019).
24. J. Yang, M. Fu, Y. Hu, "Liver vessel segmentation based on inter-scale V-Net," *Math. Biosci. Eng.* **18**, 4327–4340 (2021).
25. T. Takamoto, T. Hashimoto, S. Ogata, K. Inoue, Y. Maruyama, A. Miyazaki, M. Makuuchi, "Planning of anatomical liver segmentectomy and subsegmentectomy with 3-dimensional simulation software," *Am. J. Surg.* **206**, 530–538 (2013).
26. B. Nalbant, T. Egeli, T. Ünek, C. Altay, E. Kavur, A. Selver, F. Obuz, C. Ağalar, M. Özbilgin, İ. Astarcıoğlu, "Utilizing 3 dimensional print of the liver in living donor liver transplantation for preoperative evaluation," *J. Basic Clin. Health Sciences* **4**, 85–87 (2020).
27. C. Debbaut, P. Segers, P. Cornillie, C. Casteleyn, M. Dierick, W. Laleman, D. Monbaliu, "Analyzing the human liver vascular architecture by combining vascular corrosion casting and micro-CT scanning: A feasibility study," *J. Anat.* **224**, 509–517 (2014).
28. G. Peeters, C. Debbaut, W. Laleman, D. Monbaliu, I. Vander Elst, J. R. Detrez, T. Vandecasteele, T. De Schryver, L. Van Hoorebeke, K. Favere, J. Verbeke, P. Segers, P. Cornillie, W. H. De Vos, "A multilevel framework to reconstruct anatomical 3D models of the hepatic vasculature in rat livers," *J. Anat.* **230**, 471–483 (2017).
29. G. Peeters, C. Debbaut, A. Friebel, P. Cornillie, W. H. De Vos, K. Favere, I. Vander Elst, T. Vandecasteele, T. Johann, L. Van Hoorebeke, D. Monbaliu, D. Drasdo, S. Hoehme, W. Laleman, P. Segers, "Quantitative analysis of hepatic macro- and microvascular alterations during cirrhogenesis in the rat," *J. Anat.* **232**, 485–496 (2018).
30. S. Hankeova, J. Salplachta, T. Zikmund, M. Kavkova, N. Van Hul, A. Brinek, V. Smekalova, J. Laznovsky, F. Dawit, J. Jaros, V. Bryja, U. Lendahl, E. Ellis, A. Nemeth, B. Fischler, E. Hannezo, J. Kaiser, E. R. Andersson, "DUCT reveals architectural mechanisms contributing to bile duct recovery in a mouse model for Alagille syndrome," *eLife* **10**, e60916 (2021).
31. X. Zeng, J. Zhou, Z. Xiong, H. Sun, W. Yang, M. T. S. Mok, J. Wang, J. Li, M. Liu, W. Tang, Y. Feng, H. K. Wang, S. W. Tsang, K. L. Chow, P. C. Yeung, J. Wong, P. B. Lai, A. W. Chan, K. F. To, S. L. Chan, Q. Xia, J. Xue, X. Chen, J. Yu, S. Peng, J. J. Sung, M. Kuang, A. S. Cheng, "Cell cycle-related kinase reprograms the liver immune microenvironment to promote cancer metastasis," *Cell Mol. Immunol.* **18**, 1005–1015 (2021).
32. M. He, H. Park, G. Niu, Q. Xia, H. Zhang, B. Z. Tang, J. Qian, "Lipid droplets imaging with three-photon microscopy," *J. Innov. Opt. Health Sci.* (2022).
33. D. Deng, B. Dai, J. Wei, X. Yuan, X. Yang, S. Qi, Z. Zhang, "A drawer-type abdominal window with an acrylic/resin coverslip enables long-term intravital fluorescence/photoacoustic imaging of the liver," *Nanophotonics* **10**, 3369–3381 (2021).
34. X. Yu, L. Chen, J. Liu, B. Dai, G. Xu, G. Shen, Q. Luo, Z. Zhang, "Immune modulation of liver sinusoidal endothelial cells by melittin nanoparticles suppresses liver metastasis," *Nat. Commun.* **10**, 574 (2019).
35. L. Liu, B. Dai, R. Li, Z. Liu, Z. Zhang, "Intravital molecular imaging reveals the restrained capacity of CTLs in the killing of tumor cells in the liver," *Theranostics* **11**, 194–208 (2021).
36. S. Hammad *et al.*, "Protocols for staining of bile canalicular and sinusoidal networks of human, mouse and pig livers, three-dimensional

reconstruction and quantification of tissue microarchitecture by image processing and analysis," *Arch. Toxicol.* **88**, 1161–1183 (2014).
37. H. Wu, F. Xia, L. Zhang, C. Fang, J. Lee, L. Gong, J. Gao, D. Ling, F. Li, "A ROS-sensitive nanozyme-augmented photoacoustic nanoprobe for early diagnosis and therapy of acute liver failure," *Adv. Mater.* **34**, e2108348 (2022).
38. D. S. Richardson, J. W. Lichtman, "Clarifying tissue clearing," *Cell* **162**, 246–257 (2015).
39. E. C. Costa, D. N. Silva, A. F. Moreira, I. J. Correia, "Optical clearing methods: An overview of the techniques used for the imaging of 3D spheroids," *Biotechnol. Bioeng.* **116**, 2742–2763 (2019).
40. R. Oren, L. Fellus-Alyagor, Y. Addadi, F. Bochner, H. Gutman, S. Blumenreich, H. Dafni, N. Dekel, M. Neeman, S. Lazar, "Whole organ blood and lymphatic vessels imaging (WOBLI)," *Sci. Rep.* **8**, 1412 (2018).
41. S. Z. Dian Jing, W. Luo, X. Gao, Y. Men, C. Ma, X. Liu, Y. Yi, A. Bugde, B. O. Zhou, Z. Zhao, Q. Yuan, J. Q. Feng, L. Gao, W.-P. Ge, H. Zhao, "Tissue clearing of both hard and soft tissue organs with the PEGASOS method," *Cell Res.* **28**, 803–818 (2018).
42. K. Liu, L. Yang, G. Wang, J. Liu, X. Zhao, Y. Wang, J. Li, J. Yang, "Metabolic stress drives sympathetic neuropathy within the liver," *Cell Metab.* **33**, 666–675.e4 (2021).
43. C. Adori, T. Daraio, R. Kuiper, S. Barde, T. Hkfelt, "Disorganization and degeneration of liver sympathetic innervations in nonalcoholic fatty liver disease revealed by 3D imaging," *Sci. Adv.* **7**, eabg5733 (2021).
44. Y. Takashima, M. Terada, M. Kawabata, A. Suzuki, "Dynamic three-dimensional morphogenesis of intrahepatic bile ducts in mouse liver development," *Hepatology* **61**, 1003–1011 (2015).
45. Q. Zhang, A. Li, S. Chen, J. Yuan, T. Jiang, X. Li, Q. Luo, Z. Feng, H. Gong, "Multiscale reconstruction of various vessels in the intact murine liver lobe," *Commun. Biol.* **5**, 260 (2022).
46. S. J. Wigmore, G. C. Oniscu, "Sidestream dark field videomicroscopy for evaluating liver microcirculation *in vivo*," *Liver Transpl.* **23**, 425–426 (2017).
47. J. Bonnardel, W. T'Jonck, D. Gaublomme, R. Browaeys, C. L. Scott, L. Martens, B. Vanneste, S. De Prijck, S. A. Nedospasov, A. Kremer, E. Van Hamme, P. Borghgraef, W. Toussaint, P. De Bleser, I. Mannaerts, A. Beschin, L. A. van Grunsven, B. N. Lambrecht, T. Taghon, S. Lippens, D. Elewaut, Y. Saeys, M. Guilliams, "Stellate cells, hepatocytes, and endothelial cells imprint the kupffer cell identity on monocytes colonizing the liver macrophage niche," *Immunity* **51**, 638–654.e9 (2019).
48. S. Curio, G. T. Belz, "The unique role of innate lymphoid cells in cancer and the hepatic microenvironment," *Cell Mol. Immunol.* **19**, 1012–1029 (2022).
49. N. Méndez-Sánchez, J. Córdova-Gallardo, B. Barranco-Fragoso, M. Eslam, "Hepatic dendritic cells in the development and progression of metabolic steatohepatitis," *Front. Immunol.* **12**, 641240 (2021).
50. M. A. Freitas-Lopes, K. Mafra, B. A. David, R. Carvalho-Gontijo, G. B. Menezes, "Differential location and distribution of hepatic immune cells," *Cells* **6**, 48 (2017).
51. V. Racanelli, B. Rehermann, "The liver as an immunological organ," *Hepatology* **43**, S54–S62 (2006).
52. D. P. Bogdanos, B. Gao, M. E. Gershwin, "Liver immunology," *Compr. Physiol.* **3**, 567–598 (2013).
53. K. Si-Tayeb, F. P. Lemaigre, S. A. Duncan, "Organogenesis and development of the liver," *Dev. Cell* **18**, 175–189 (2010).
54. C. N. Jenne, P. Kubes, "Immune surveillance by the liver," *Nat. Immunol.* **14**, 996–1006 (2013).
55. T. Matsumoto, L. Wakefield, B. D. Tarlow, M. Grompe, "*In vivo* lineage tracing of polyploid hepatocytes reveals extensive proliferation during liver regeneration," *Cell Stem Cell* **26**, 34–47.e3 (2020).
56. T. Nishio, R. Hu, Y. Koyama, S. Liang, S. B. Rosenthal, G. Yamamoto, D. Karin, J. Baglieri, H. Y. Ma, J. Xu, X. Liu, D. Dhar, K. Iwaisako, K. Taura, D. A. Brenner, T. Kisseleva, "Activated hepatic stellate cells and portal fibroblasts contribute to cholestatic liver fibrosis in MDR2 knockout mice," *J. Hepatol.* **71**, 573–585 (2019).
57. I. Mederacke, C. C. Hsu, J. S. Troeger, P. Huebener, X. Mu, D. H. Dapito, J. P. Pradere, R. F. Schwabe, "Fate tracing reveals hepatic stellate cells as dominant contributors to liver fibrosis independent of its aetiology," *Nat. Commun.* **4**, 2823 (2013).
58. A. H. Lau, A. W. Thomson, "Dendritic cells and immune regulation in the liver," *Gut* **52**, 307–314 (2003).
59. E. Lafoz, M. Ruart, A. Anton, A. Oncins, V. Hernández-Gea, "The endothelium as a driver of liver fibrosis and regeneration," *Cells* **9**, 929 (2020).
60. A. Maretti-Mira, L. DeLeve, "Liver sinusoidal endothelial cell: An update," *Semin. Liver Dis.* **37**, 377–387 (2017).
61. A. Gola, M. G. Dorrington, E. Speranza, C. Sala, R. M. Shih, A. J. Radtke, H. S. Wong, A. P. Baptista, J. M. Hernandez, G. Castellani, I. D. C. Fraser, R. N. Germain, "Commensal-driven immune zonation

of the liver promotes host defence," *Nature* **589**, 131–136 (2021).
62. M. de Krijger, M. E. Wildenberg, W. J. de Jonge, C. Y. Ponsioen, "Return to sender: Lymphocyte trafficking mechanisms as contributors to primary sclerosing cholangitis," *J. Hepatol.* **71**, 603–615 (2019).
63. B. Zheng, J. Zhang, H. Chen, H. Nie, H. Miller, Q. Gong, C. Liu, "T lymphocyte-mediated liver immunopathology of schistosomiasis," *Front. Immunol.* **11**, 61 (2020).
64. K. Yu, P. Li, T. Xu, J. Xu, K. Wang, J. Chai, D. Zhao, Y. Liu, Y. Wang, J. Ma, L. Fan, S. Guo, Z. Li, M. Li, Z. Wang, "Decreased infiltration of CD4(+) Th1 cells indicates a good response to ursodeoxycholic acid (UDCA) in primary biliary cholangitis," *Pathol. Res. Pract.* **217**, 153291 (2021).
65. N. Pishesha, T. J. Harmand, H. L. Ploegh, "A guide to antigen processing and presentation," *Nat. Rev. Immunol.* **22**, 751–764 (2022).
66. T. Gebhardt, U. Palendira, D. C. Tscharke, S. Bedoui, "Tissue-resident memory T cells in tissue homeostasis, persistent infection, and cancer surveillance," *Immunol. Rev.* **283**, 54–76 (2018).
67. S. Ghilas, A. M. Valencia-Hernandez, M. H. Enders, W. R. Heath, D. Fernandez-Ruiz, "Resident memory T cells and their role within the liver," *Int. J. Mol. Sci.* **21**, 8565 (2020).
68. C. Khairallah, T. H. Chu, B. S. Sheridan, "Tissue adaptations of memory and tissue-resident gamma delta T cells," *Front. Immunol.* **9**, 2636 (2018).
69. L. Hammerich, F. Tacke, "Role of gamma-delta T cells in liver inflammation and fibrosis," *World J. Gastrointest. Pathophysiol.* **5**, 107–113 (2014).
70. G. Gasteiger, X. Fan, S. Dikiy, S. Y. Lee, A. Y. Rudensky, "Tissue residency of innate lymphoid cells in lymphoid and nonlymphoid organs," *Science* **350**, 981–985 (2015).
71. D. K. Sojka, Z. Tian, W. M. Yokoyama, "Tissue-resident natural killer cells and their potential diversity," *Semin. Immunol.* **26**, 127–131 (2014).
72. V. Kumar, T. L. Delovitch, "Different subsets of natural killer T cells may vary in their roles in health and disease," *Immunology* **142**, 321–336 (2014).
73. B. A. David, R. M. Rezende, M. M. Antunes, M. M. Santos, M. A. Freitas Lopes, A. B. Diniz, R. V. Sousa Pereira, S. C. Marchesi, D. M. Alvarenga, B. N. Nakagaki, A. M. Araujo, D. S. Dos Reis, R. M. Rocha, P. E. Marques, W. Y. Lee, J. Deniset, P. X. Liew, S. Rubino, L. Cox, V. Pinho, T. M. Cunha, G. R. Fernandes, A. G. Oliveira, M. M. Teixeira, P. Kubes, G. B. Menezes, "Combination of mass cytometry and imaging analysis reveals origin, location, and functional repopulation of liver myeloid cells in mice," *Gastroenterology* **151**, 1176–1191 (2016).
74. F. Sierro, M. Evrard, S. Rizzetto, M. Melino, A. J. Mitchell, M. Florido, L. Beattie, S. B. Walters, S. S. Tay, B. Lu, L. E. Holz, B. Roediger, Y. C. Wong, A. Warren, W. Ritchie, C. McGuffog, W. Weninger, D. G. Le Couteur, F. Ginhoux, W. J. Britton, W. R. Heath, B. M. Saunders, G. W. McCaughan, F. Luciani, K. P. A. MacDonald, L. G. Ng, D. G. Bowen, P. Bertolino, "A liver capsular network of monocyte-derived macrophages restricts hepatic dissemination of intraperitoneal bacteria by neutrophil recruitment," *Immunity* **47**, 374–388.e6 (2017).
75. M. Guilliams, J. Bonnardel, B. Haest, B. Vanderborght, C. Wagner, A. Remmerie, A. Bujko, L. Martens, T. Thoné, R. Browaeys, F. F. De Ponti, B. Vanneste, C. Zwicker, F. R. Svedberg, T. Vanhalewyn, A. Gonçalves, S. Lippens, B. Devriendt, E. Cox, G. Ferrero, V. Wittamer, A. Willaert, S. J. F. Kaptein, J. Neyts, K. Dallmeier, P. Geldhof, S. Casaert, B. Deplancke, P. Ten Dijke, A. Hoorens, A. Vanlander, F. Berrevoet, Y. Van Nieuwenhove, Y. Saeys, W. Saelens, H. Van Vlierberghe, L. Devisscher, C. L. Scott, "Spatial proteogenomics reveals distinct and evolutionarily conserved hepatic macrophage niches," *Cell* **185**, 379–396.e38 (2022).
76. E. Kolaczkowska, C. N. Jenne, B. G. Surewaard, A. Thanabalasuriar, W. Y. Lee, M. J. Sanz, K. Mowen, G. Opdenakker, P. Kubes, "Molecular mechanisms of NET formation and degradation revealed by intravital imaging in the liver vasculature," *Nat. Commun.* **6**, 6673 (2015).
77. C. Pan, R. Cai, F. P. Quacquarelli, A. Ghasemigharagoz, A. Lourbopoulos, P. Matryba, N. Plesnila, M. Dichgans, F. Hellal, A. Ertürk, "Shrinkage-mediated imaging of entire organs and organisms using uDISCO," *Nat. Methods* **13**, 859–867 (2016).
78. S. I. Kubota, K. Takahashi, J. Nishida, Y. Morishita, S. Ehata, K. Tainaka, K. Miyazono, H. R. Ueda, "Whole-body profiling of cancer metastasis with single-cell resolution," *Cell Rep.* **20**, 236–250 (2017).